1979, *Astron. Astrophys. Suppl.* **36**, 323-330.

THE DETECTION OF PLANETARY NEBULAE NEAR THE GALACTIC CENTRE AT RADIO WAVELENGTHS. I

J.G.A. WOUTERLOOT and E. DEKKER
Sterrewacht, Leiden, The Netherlands

Received May 22, 1978, revised October 27, 1978

During a search at 1415 MHz near the galactic centre 123 sources have been detected, 14 of which are identified with optically known planetary nebulae, mostly at the distance of the galactic centre. Out of the 109 remaining sources we predict that probably 85 are extragalactic background sources. The remaining 24 sources we interpret as a collection of optically invisible planetary nebulae and compact H II regions. The number of sources per unit area increases towards the galactic centre. If interpreted as planetary nebulae the distribution is roughly what one expects from other information on the galactic centre.

Key words: radio sources – planetary nebulae – galactic centre

1. INTRODUCTION

For a better understanding of the regions around the galactic centre, knowledge of the distribution of well-evolved stars is likely to be of great importance (Oort, 1977a). Such a knowledge will help not only in a more secure determination of the mass-distribution in the galactic centre, but also in an improved understanding of the recirculation of matter. Unfortunately, optical observations are not at all useful in finding the distribution of well-evolved stars, because of the large extinction by interstellar dust. Only longward of 2 μm the extinction is sufficiently small to enable observations. Several infrared studies have been made (e.g. Becklin *et al.*, 1978). Radio observations offer other possibilities. There are at least two types of well-evolved stars that emit sufficient radio emission to be observable even at the distance of the galactic centre: OH/IR stars (Baud *et al.* 1979) and planetary nebulae. The present paper describes the positive results of a pilot program to detect planetary nebulae near the galactic centre with the Westerbork Synthesis Radio Telescope.

2. OBSERVATIONS

The WSRT has been described by Baars and Hooghoudt, 1974; Högbom and Brouw, 1974; Casse and Muller, 1974 and van Someren Gréve, 1974. In the direction of the galactic centre ($\delta = -29°$) the WSRT antenna pattern is elongated in declination and has large negative side lobes in right ascension. This latter feature is a consequence of the fact that at low declinations the observations can cover only an hour angle range of 4^h, thus giving a partly synthesized beam. It has a half-power width of about $20'' \times 120''$ in α and δ, respectively.

Six fields of 40 arcmin diameter were observed in the continuum at 1415 MHz during the period from October 1974 until March 1976. These fields were selected using two criteria: firstly, they had to be close to, but at different angular distances from the galactic centre and, secondly, they had to contain as many as possible of the optically-known planetary nebulae listed in the catalogue of Perek and Kohoutek (1967). The second criterion ensures that some information could be obtained about the radio luminosity function of planetary nebulae. Relevant parameters of the different fields are shown in table 1, which is organized as follows: column (1) field number; (2), (3) α and δ (1950) of the field centre; (4) distance r from field centre to galactic centre in degrees; (5) observed spacings: 90 (72) 1458 means spacing 90 m to 1458 m observed in steps of 72 m; (6) number 4^h observations; (7) resulting rms noise (mJy) for a point source in the centre of the field. Fields 1 and 2 have been observed during 1×4^h, fields 3, 4 and 5 were extended to 4×4^h to lower the noise. Field 6 was observed 8×4 hours to get rid of the grating rings of Sgr A, which was near the edge of the field.

3. REDUCTION AND RESULTS

Two different maps have been made of each field using standard procedures. The maps differ in the way the various interferometer responses have been weighted. In the first map (called "a") all baselines were used and in the second map (called "b") only baselines longer than 500 m were used. A comparison between the two maps enables us to detect the presence of extended sources and to recognize point sources within the fields. Grating ring responses due to strong or extended sources were removed from the maps using "subtract" or "clean" procedures in order to enable us to find weaker sources. Due to the presence of Sgr A in field 6 many point sources were partially hidden on map (a) behind extended emission or sidelobes. This could not be improved by cleaning, so we used map (b) to get the parameters of the sources. For the extended sources we used map (a). The same procedure was also followed for the other fields to get uniform results. All observations were done at low elevations (4°–10°). As a result of the relative large atmospheric extinction and a total power increase due to atmospheric emission, the measured flux densities were somewhat too low. We applied a best estimated correction to them. It amounted from 15% in field 4, 20% in field 1, 2, 3 and 5 to 30% in field 6. The uncertainty in flux density mentioned in table A1 may be in reality in some cases a factor 2 higher.

The observed sources in the different fields are listed in table A1 of the appendix.

4. ANALYSIS

Optically known planetary nebulae

The observed fields contained 25 optically known planetary nebulae (P & K = Perek and Kohoutek 1967). In many cases the optical positions are not very accurate in P & K. Some Hα and red continuum plates were taken by A.G. de Bruyn with the 48-inch Schmidt telescope at Mt. Palomar. The positions of all the nebulae visible on the plates and listed in P & K were measured on film copies of the Hα plates with an $x-y$ measuring machine at Leiden Observatory to an accuracy of 0.″5 in α and δ. The measured positions together with other information about the nebulae are shown in table 2. Differences of individual positions with respect to the nearest position in P & K are in the last column. In most cases the best position in P & K is from Kohoutek *et al.* (1965). The criterion for an identification has been that the difference between optical and radio position in α and δ is much smaller than the synthesized beam. In many cases (cf. columns 4 and 5) this difference is larger than the error in radioposition quoted in table A1, but this latter may be a lower limit due to the low declination. Of the 25 planetary nebulae 14 have been detected by the WSRT. These detections and the upper limits of the undetected nebulae are also shown in table 2. Several of the detected nebulae have such high radial velocities that they must be at the galactic centre.

Optical candidates for identification

The Hα plates obtained by de Bruyn have been used to search for possible optical candidates at the positions of the radio sources. We could do this only for the fields 3 and 6 (the other fields are too crowded with stars). In field 3 three optical objects were identified out of a total of 27 radio source positions. In field 6 we identified 8 optical objects out of 32 positions. The results are shown in table 3.

In order to estimate the probability of spurious identifications we determined the mean star density on the plates ($5.5\ 10^{-4}$ arcsec^{-2} and $18\ 10^{-4}$ arcsec^{-2} for field 3 and 6 respectively). For these fields the expected number of stellar objects within error boxes ($\Delta\alpha = 2.''5$, $\Delta\delta = 7''$) are 0.8 and 3. Of the coincidences between radio and optical objects in table 3, a large fraction is thus expected to be real. For one of the sources in table 3 additional material confirms that it is a new planetary nebulae. The optical object that coincides with the radio sources 19W32 has an extended structure in Hα with an angular size of about 24″. A spectrum taken by A.G. de Bruyn (private communication) shows the [0 III] line at 5007 Å. The objects, when placed at the galactic centre would have a linear dimension of 1.1 pc, where is somewhat large for a typical planetary nebulae. If indeed the object is a planetary nebulae, it probably is a foreground object.

The radio luminosity function of planetary nebulae.

Very little is known about the radio luminosity function of planetary nebulae. Therefore we selected the fields in such a way that they contained as many as possible optically known nebulae. Since the distribution of planetary nebulae in galactic longitude shows a strong concentration towards the galactic centre it seems plausible that most of the known planetaries within 5° from the galactic centre will be at the distance of the centre. From a comparison of the number of planetary nebulae away from the centre and towards it, we estimate that the number of foreground sources in our sample is less than 10% the total.

In figure 1 a histogram of the observed radio flux density distribution for the fourteen optically known planetary nebulae taken from table 4 is shown (the open area). The hatched area indicates upper limits of the not detected nebulae. We realize that several selection effects may severely influence the form of the distribution function of the galactic centre. Among these is the before mentioned effect of foreground nebulae which, although small in number, might affect the high luminosity tail of the distribution. For instance, the brightest nebulae in the sample is PK 3 – 4.5 (NGC 6565) which is almost certainly such a foreground nebulae. It has an angular extent of $19'' \times 8''$ and a small radial velocity (−5 km s).

Another selection effect is that planetary nebulae with low radio luminosity are expected to have low optical surface brightness and hence difficult to detect because of interstellar extinction.

The surface density of radio sources

We derived the surface density of radio sources as a function of the angular distance r to the galactic centre by counting sources in limited areas of our fields. These counts have been made in several ways.

In fields 3, 4 and 5 we have counted sources according to two different criteria:

a) all sources within 0°.4 of the field centre and brighter than 6.5 mJy (uncorrected for primary beam attenuation).

b) all sources within 0°.55 of the field centre and brighter than 3.6 mJy (uncorrected for primary beam attenuation).

In field 6 we followed a different procedure, because this field is closest to the galactic centre, and hence a density gradient across the field may be expected. Therefore we divided an area within 0°.4 of the centre of field 6 into two equal sections with mean distances from the galactic centre of respectively 0°.84 and 0°.48. In these two sections we then counted all sources brighter than 6.5 mJy (uncorrected for primary beam attenuation), consistent with criterion (a) for the other fields.

The results of these counts are given in table 4 where in column 3 and 4 results are given for criterion (a) and (b) respectively.

The counts contain planetary nebulae, (compact) H II regions and extragalactic background sources. There is at present no (radio astronomical) method available to separate planetary nebulae from H II regions; the background sources can be weeded out because of the non-thermal spectra. However, at the moment we lack the required observations at other wavelengths. Therefore we estimate the number of extragalactic background objects in a statistical way.

From differential counts from surveys done with the WSRT at 1415 MHz, Willis *et al.* (1977) derived the relation

$$\frac{dN}{dS} = 310.72\, S^{(-2.59-0.106 \ln S)},$$

where N is the number of sources per sterad and S the flux density in Jy. Although this relation has been obtained with a rather different beam shape, it may be sufficiently accurate for the present purpose. When integrated over $S > 6.5$ mJy it yields about 9 background sources within 0°.4 from the field centre. Doing the same for $S > 3.6$ mJy we obtain 19 sources within 0°.55. From table 4 we can conclude that in each of the fields 3, 6A, 6B, there is a clear surplus of sources, which is increasing towards the centre. It probably consists of planetary nebulae but some sources may be compact H II regions.

5. DISCUSSION

The increasing number density of planetary nebulae towards the galactic centre has been discussed by Oort (1977b), who found that the radial velocities of 64 planetaries within 0.7 kpc from the centre fitted closely a Maxwellian velocity distribution with a dispersion of 125 km s^{-1}. The correction for the effect of foreground nebulae yielded a true dispersion of 134 km s^{-1}. From the distributions of radial velocities of type II OH masers, probably a category of objects related to planetary nebulae, Baud *et al.* (1979) obtain a velocity dispersion of 130 ± 20 km s^{-1}. Using data on the gravitational potential field as indicated by the rotation of the H I nuclear disk, Oort concluded that between $R=0.08$ kpc and $R=1.0$ kpc (where R is the distance to the galactic centre) the spatial density of planetary nebulae should vary as $R^{-2.9}$. The surface density σ is therefore expected to vary as $R^{-1.9}$. In figure 2 we have plotted log σ against log R for the radio sources observed in the direction of the galactic centre, (corrected for background sources, see table 4, column 5). We deduce from these data a value for $d \log \sigma / d \log R$ of $-1.23^{+0.5}_{-0.9}$.

If we take for the dispersion in radial velocity 134 km s^{-1} we can conclude from this gradient that the circular velocity at 200 pc from the galactic centre is about 200 km s^{-1}, instead of the value of 230 km s^{-1} as adopted by Oort. However, we stress that this result is quite uncertain.

The greatest source of uncertainty is the small number of sources involved, but another source of uncertainty is the statistical correction for background sources. Obviously the result can be considerably improved with higher sensitivity 21 cm observations to find more sources and additional 6 cm observations to separate thermal from non-thermal sources. This will be the aim of a new program, already started.

6. CONCLUSIONS

We have detected radio continuum sources in 6 fields near the galactic centre with the WSRT at 21 cm. The surface density of these sources increases towards the galactic centre and is clearly in excess over that of extra galactic background sources. Of all radio sources 14 coincide with optically known planetary nebulae in the fields. The radial velocity of several nebulae indicates that they must be at the galactic centre. We therefore assume that the excess of radio sources is largely due to planetary nebulae that have not been observed optically because of interstellar extinction.

On the basis of a simplified spherical model for the distribution of mass near the galactic centre we relate the rate of increase of the excess of radio sources to the gravitational potential near the galactic centre. Our result indicates that the potential between 100 and 300 pc from the galactic centre is somewhat smaller than concluded from H I observations, but the difference is only marginally significant.

We have thus demonstrated that it is possible to study the population of planetary nebulae near the galactic centre. This paper is the result of a pilot program carried out with the WSRT. A more extended observing program with higher sensitivity has been started in the expectation of obtaining larger numbers of sources, and of obtaining data by which the background sources can be eliminated.

ACKNOWLEDGEMENTS

We thank J.H. Oort, H.J. Habing and R.D. Ekers, who suggested the program, for their stimulating discussions. A.G. de Bruyn kindly provided the Hα plates for us. We greatfully acknowledge the advice for reducing the data given by W.W. Shane and A.G. de Bruyn.

The Westerbork Synthesis Radio Telescope is operated by the Netherlands Foundation for Radio Astronomy with the financial support of the Netherlands Organization for the Advancement of Pure Research (Z.W.O.)

REFERENCES

Baars, J.W.M. and Hooghoudt, B.G.: 1974, *Astron. & Astrophys.* **31**, 323.
Baud, B., Habing, H.J., Matthews, H.E. and Winnberg, A.: 1979, to be published in *Astron. & Astrophys.*
Beard, M., Thomas, B.MacA. and Day, G.A.: 1969, *Aus. J. Phys. Suppl.* **11**, 27.
Becklin, E.E., Neugebauer, G. and Early, D.: 1978, in preparation.
Casse, J.L. and Muller, C.A.: 1974, *Astron. & Astrophys.* **31**, 333.
Dixon, R.S.: 1970, *Astrophys. J. Suppl.* **180**, 503.
Ehman, J.R., Dixon, R.S. and Kraus, J.D.: 1970, *Astron. J.* **75**, 351.
Gardner, F.F. and Whiteoak, J.B.: 1975, MNRAS **171**, 29P.
Högbom, J.A. and Brouw, W.N.: 1974, *Astron. & Astrophys.* **33**, 289.
Joshi, M.N., Kapahi, V.K., Gopal-Krishna, Sarma, N.V.G. and Swarup, G.: 1973, *Astron. J.* **78**, 1023.
Kesteven, M.J.L.: 1968, *Astr. J. Phys.* **21**, 369.
Milne, D.K. and Aller, L.H.: 1975, *Astron. & Astrophys.* **38**, 183.
Minkowski, R.: 1968, *Publ. Astron. Soc. Pacific* **76**, 197.
Oort, J.H.: 1971, *Les Noyeaux des Galaxies, Pont. Ac. Sc. Scripta Varia* **35**, 321.
Oort, J.H.: 1977a, *Ann. Rev. of Astron. and Astrophys.* **15**, 295.
Oort, J.H.: 1977b, *Astrophys. J. Letters* **218**, L97.
Perek, L. and Kohoutek, L.: 1967, *Catalogue of galactic planetary nebulae* (Academia Publ. House, Prague).
Rougoor, W.G. and Oort, J.H.: 1960, *Proc. Nat. Ac. Sc. Washington* **46**, 1.
Someren Gréve, H.W. van: 1974, *Astron. Astrophys. Suppl.* **15**, 343.
Whiteoak, J.B. and Gardner, F.F.: 1973, *Astrophys. J. Letters* **13**, 205.
Willis, A.G., Oosterbaan, C.E., Le Poole, R.S., Ruiter, H.R. de, Strom, R.G., Valentijn, E.A., Katgert, P. and Katgert-Merkelijn, J.H.: 1977, *Proc. I.A.U. Symp. 74.*

J.G.A. Wouterloot
E. Dekker

Sterrewacht
Postbus 9513
2300 RA Leiden
The Netherlands

APPENDIX

Observed radio sources

Table A1 shows the detected sources in the different fields. It is organized as follows:
Column (1) name of source (the sources are named according to the new WSRT nomenclature); (2), (3) α and δ 1950); (4) flux density (mJy) corrected for primary beam attenuation; (5) primary beam attenuation; (6) distance from field centre in degrees; (7) comments.

Previously known radio sources

Among the sources detected there are several that have been observed before. For comparison we have listed in table A2 the previously known sources in the fields as given by Dixon (1970, edition 1974). When in our fields a source was found near the given position it was included in table A2. All previous observations were done with much larger beam sizes. Therefore comparison of the flux densities is difficult. Of the sources mentioned in table A2 only one could be compared directly namely NGC 6565. For this source the agreement between the present and earlier (Milne & Aller 1975) observations is good.

OTL 1725–287 (Joshi *et al.* 1973) is a complex, possibly double source whose centre coincides with the position of 19W84.

KES54 probably can be identified with the point source 19W40; Kesteven (1968) quotes a size for KES54 of 3$'$.6, but only very weak extended emission can be seen on our maps. The flux density is abnormally low in comparison with that of Kesteven; the spectral index seems to be steeper than -2. Clearly, observations at longer wavelengths are necessary.

The source of 19W118 probably consists of two parts. First a central pointlike source which is mentioned in table A1. Second a region of more extended emission which coincides with BTD 0.4–0.8 (see table A2).

The source BTD 0.6–0.9, identified with the H II region RCW 142 (Beard *et al.* 1969), is resolved into two separate point sources. One (19W121) coincides with the position given for BTD 0.6–0.9; the other (19W123) coincides with RCW 142. The two sources are situated near the edge of field 6, so the flux density is rather uncertain. Gardner and Whiteoak (1975) found a type I OH maser near RCW 142. It is not clear what the exact position is with respect to RCW 142.

OU–216 was incompletely mapped by Ehman *et al.* (1970). It probably consists of the 3 sources 19W55, 19W57 and 19W59. The total flux density of these 3 sources is 1.06 Jy, about the same as the flux density of OU–216.

Table 1 observed fields

(1) field number	(2) α (1950.0)	(3) δ (1950.0)	(4) r (degrees)	(5) telescope spacings	(6) number of 4^h observations	(7) r.m.s. noise (mJy)
1	17 22.8	−29 19.3	4.31	90(72)1458	1	2.4
2	17 54.5	−29 52.2	2.79	90(72)1458	1	2.4
3	17 35.9	−28 43.5	1.46	36(18)1458	4	0.8
4	18 08.5	−28 05.0	5.79	36(18)1458	4	0.8
5	17 24.8	−28 31.4	3.89	36(18)1458	4	0.8
6	17 45.0	−29 16.0	0.61	36(09)1467	8	1.3

Table 4 Source counts

(1) field number	(2) r (degrees)	(3)* N(a)	(4)* N(b)	(5)** $N_{corr.}$(a)	(6)** $N_{corr.}$(b)
4	5.79	8	19	−1 ± 3	0 ± 4
5	3.89	10	22	1 ± 3	3 ± 4
3	1.46	14	24	5 ± 3	5 ± 4
6A	0.84	16	-	7 ± 4	-
6B	0.48	24	-	15 ± 5	-

* N = number of sources detected.
** $N_{corr.}$ = number of sources after correction for extragalactic background contributions.

Table 2 Optically known planetary nebulae

(1) PeK	(2) α (1950.0)	(3) δ (1950.0)	(4) $(\Delta\alpha)_1$	(5) $(\Delta\delta)_1$	(6) S_{1415} (mJy)	(7) V_{rad} kms^{-1}	(8) $(\Delta\alpha)_2$	(9) $(\Delta\delta)_2$	(10) ref.
357+3.1	17 21 23.44	−29 21 37.6	0.03	− 5.0	31.5	−191	−0.1	0	Koal
357+3.3	17 24 21.51	−29 00 25.1			< 5				I
357+3.4	17 23 49.07	−29 13 01.3	0.47	14.5	9.4	−250	−0.1	−1	Koal
357+3.5	17 24 13.43	−29 18 44.2			< 12		0	0	Koal
358+2.1	17 28 03.81	−28 21 09.2					−0.9	50	Fc
358+3.1	17 24 10.64	−28 25 22.1	0.05	5.1	33.2	− 94	0	0	Koal
358+3.2	17 24 23.12	−28 28 38.6	−0.04	1.3	17.4	+ 50	−0.1	0	Koal
358+3.3	17 25 32.17	−28 24 55.7	0.07	12.9	4.8				I
358+3.4	17 26 53.59	−27 57 00.3				+ 65	−0.1	0	Koal
358+3.5	17 25 17.00	−28 36 10.8			<4.2		−0.1	−2	Koal
358+3.6	17 27 34.65	−28 01 52.6				+168	−0.1	−2	Koal
358+3.7	17 26 30.56	−28 38 02.3	0.06	− 0.9	6.8	+ 1	−0.1	+1	Koal
358+3.8	17 26 59.80	−28 12 36.6					0.3	11	Koal
359−0.1	17 44 43.97	−29 58 43.1				− 28	0.1	−4	Koal
359+1.1	17 35 32.01	−28 41 05.8	0.12	5.5	17.3				I
359+1.2	17 36 10.42	−28 45 24.7			< 4				I
000−2.6	17 55 05.61	−29 59 56.2	−1.64	− 1.5	9.6	+158	−1.5	31	Koal*
000−2.5	17 54 29.27	−30 01 45.2			< 8				I
000−2.4	17 54 57.8	−29 44 06	0.15	2.6	26.6	−127			Koal**
000−2.3	17 53 12.39	−29 37 42.1			< 14	+145	−0.3	2	Koal
000−1.1	17 47 12.85	−29 24 31.0	−0.04	13.7	30.9	+ 20	0.1	−2	Koal
000−0.2	17 43 46.67	−28 59 38.8			< 6		−5.1	16	WHal
000−0.1	17 43 58.94	−28 45 26.7			< 13		−1.1	−4	WHal
.003−4.9	18 09 38.16	−28 20 48.8			< 6		0	0	Koal
003−4.8	18 09 25.20	−27 58 58.9	0.14	− 4.8	16.0	+174	−0.3	2	Koal
003−4.7	18 08 25.25	−28 23 20.0	−0.13	− 5.0	7.1		0	0	Koal
003−4.6	18 07 51.56	−28 33 20.4			< 4.5		0	1	Koal
003−4.5	18 08 43.05	−28 11 27.1	0.20	2.8	47.3	− 5	0	0	Koal
003−4.4	18 09 14.71	−27 53 02.3			< 4.5		0	−1	Koal
003−4.3	18 08 20.24	−27 46 58.7	0.09	−26.1	4.7		−0.1	0	Koal
004 4.1	18 09 16.71	−27 30 00.4					0.5	−18	Koal

Table 2 References

Column (1) designation
(2) α (1950), measured optical position
(3) δ (1950), measured optical position
(4) α (optical – radio), (seconds)
(5) δ (optical – radio), (arcseconds)
(6) 1415 MHz Flux density, mJy
(7) radial velocity, km/s (from P & K)
(8) difference between α as measured by us and as given by P & K (seconds)
(9) difference between δ as measured by us and as given by P & K (arcseconds)
(10) Reference about nearest position in P & K:
Koal = Kohoutek, L., Pekny, Z. and Perek, L., 1965, Bull. Astron. Inst. Czechoslovakia; **16**, 189
Fc = Francman, L., 1962, Astron. Zh. Akad. Nauk. SSSR, **39**, 256
WHal = Wehninger, P.A., Rubin, R. and Blanco, V.M., 1964, private communication to P & K;
I = position improved in accuracy with respect to P & K;
* = possible wrong identification. No Hα plate available;
** = position by Koal. No Hα plate available; on PSS print no identification.

Table 3 Optical candidates in the fields 3 and 6

	(1) source name	(2) α(1950)	(3) δ(1950	(4) Δα	(5) Δδ	(6)
3a	19W25	17 35 05.55	−29 09 05.4	1.2	5.7	0.3
3b	19W27	17 35 32.01	−28 41 05.8	1.2	4.4	1.8
3c	19W32	17 35 52.34	−28 54 57.3	1.2	5.0	0.8
6a	19W95	17 43 44.28	−29 26 48.4	1.8	7.8	1.4
6b	19W96	17 43 56.51	−28 44 59.9	1.2	4.7	1.1
6c	19W97	17 44 01.39	−29 28 14.8	1.2	3.8	1.0
6d	19W98	17 44 07.34	−29 26 38.6	1.1	3.6	1.0
6e	19W101	17 44 42.75	−28 50 44.9	1.1	3.6	1.5
6f	19W121	17 47 03.33	−28 53 39.6	1.0	3.6	2.3
6g	19W122	17 47 12.85	−29 24 31.0	1.4	8.2	1.7
6h	19W123	17 47 13.6	−28 52 35	1.3	6.0	-

column (1) name of source
column (2) optical α (1950)
column (3) optical δ (1950)
column (4) combined optical and radio position uncertainty in α, arcseconds
column (5) combined optical and radio position uncertainty in δ, arcseconds
column (6) difference in optical and radio position, sigma

3b is the planetary nebulae 359 + 1.1
3c shows a remarkable difference between Hα and continuum plate and is possibly a planetary nebulae.
6a is an extended radio source
6b is situated within weak Hα emission – possible PN or H II region
6g is the planetary nebulae 0–1.1
6h is the H II region RCW 142.

Table A1 Detected sources

(1) Source name	(2) α (1950.0)	(3) δ (1950.0)	(4) flux density (mJy)	(5) atten.	(6) distance from field centre (degrees)	(7)* comments
Field 1.						
19W1	17 21 09.85 0.08	-28 58 36.4 5.3	119.3 12.8	6.50	0.50	
19W2	17 21 23.41 0.09	-28 21 32.3 6.0	31.5 2.4	2.01	0.31	PN
19W3	17 21 31.58 0.09	-29 04 32.4 6.4	39.1 3.4	2.76	0.38	
19W4	17 21 54.09 0.08	-29 44 56.9 5.3	98.2 9.6	5.23	0.47	
19W5	17 22 23.87 0.08	-29 23 23.1 3.8	45.3 1.3	1.09	0.11	
19W6	17 22 48.82 0.09	-29 19 31.6 7.8	10.7 1.0	1.00	0.00	
19W7	17 23 05.83 0.08	-29 07 56.6 4.7	30.9 1.6	1.31	0.20	
19W8	17 23 48.60 0.13	-29 13 15.8 12.4	9.4 1.4	1.49	0.24	PN
19W9	17 24 00.50 0.09	-29 14 08.3 6.4	24.8 1.9	1.70	0.27	
19W10	17 24 57.07 0.09	-29 11 54.4 6.4	79.3 8.8	5.67	0.48	
Field 2.						
19W11	17 52 59.95 0.09	-30 04 42.2 6.0	40.6 3.5	2.83	0.38	
19W12	17 53 32.00 0.09	-29 51 29.4 6.4	17.0 1.3	1.33	0.20	
19W13	17 53 58.69 0.09	-29 29 06.2 6.0	45.4 4.0	3.18	0.40	
19W14	17 54 18.37 0.07	-29 54 01.8 3.6	69.9 1.2	1.01	0.05	
19W15	17 54 23.88 0.09	-29 55 17.1 6.0	13.8 1.0	1.01	0.05	
19W16	17 54 57.65 0.08	-29 44 08.6 4.7	26.6 1.3	1.23	0.17	PN
19W17	17 55 07.25 0.11	-29 59 54.7 9.7	9.6 1.5	1.28	0.19	PN
Field 3.						
19W18	17 33 10.95 0.08	-28 34 04.0 4.7	246.4 22.2	18.67	0.61	
19W19	17 33 25.20 0.09	-28 58 21.0 6.7	114.0 13.7	15.83	0.59	
19W20	17 34 17.41 0.10	-28 53 20.3 8.2	16.2 1.8	2.84	0.38	
19W21	17 34 17.57 0.09	-29 06 12.3 6.4	57.6 6.6	7.39	0.51	
19W22	17 34 55.88 0.12	-28 49 18.3 3.8	5.8 0.7	1.42	0.22	
19W23	17 34 59.10 0.09	-28 37 43.8 8.2	8.1 0.7	1.37	0.21	
19W24	17 35 05.32 0.08	-28 50 52.7 3.8	28.1 1.1	1.35	0.21	
19W25	17 35 05.57 0.08	-29 09 06.7 5.7	46.5 4.4	4.78	0.46	
19W26	17 35 17.10 0.09	-28 48 23.4 13.9	9.7 0.6	1.16	0.15	
19W27	17 35 31.89 0.08	-28 41 00.3 4.4	17.3 0.6	1.04	0.08	PN
19W28	17 35 33.75 0.13	-28 42 40.8 12.4	3.7 0.6	1.02	0.07	
19W29	17 35 46.43 0.11	-28 56 27.9 9.7	6.6 0.6	1.39	0.22	
19W30	17 35 49.04 0.09	-28 44 49.2 6.7	7.4 0.5	1.00	0.02	
19W31	17 35 52.26 0.12	-28 30 15.2 10.8	5.9 0.7	1.40	0.22	
19W32	17 35 52.29 0.08	-28 54 59.3 5.0	14.4 0.8	1.30	0.20	
19W33	17 36 02.52 0.07	-28 45 25.5 3.4	98.9 1.4	1.02	0.05	
19W34	17 36 04.39 0.12	-28 23 52.3 11.2	9.0 1.2	2.20	0.33	
19W35	17 36 07.53 0.09	-28 46 00.5 7.1	7.1 0.6	1.04	0.07	
19W36	17 36 17.38 0.12	-28 04 44.7 10.8	98.4 12.4	23.43	0.66	
19W37	17 36 21.05 0.08	-28 42 03.9 4.7	32.9 3.6	1.08	0.11	E 68"0°
19W38	17 36 27.87 0.07	-28 32 11.3 3.6	76.3 2.8	1.46	0.23	
19W39	17 36 34.32 0.11	-28 46 22.2 10.4	5.4 0.6	1.21	0.17	
19W40	17 36 57.56 0.07	-28 40 31.6 3.4	191.7 5.9	1.54	0.25	
19W41	17 37 22.54 0.09	-28 32 34.9 6.7	20.9 1.9	2.83	0.38	
19W42	17 37 22.55 0.09	-28 42 31.0 6.4	15.7 1.4	2.22	0.34	
19W43	17 37 24.66 0.09	-28 40 03.4 6.7	17.3 1.6	2.36	0.35	
19W44	17 37 31.17 0.07	-28 46 41.7 3.6	96.8 5.8	2.67	0.37	
Field 4.						
19W45	18 07 23.38 0.11	-28 00 09.2 10.8	6.3 0.8	1.59	0.26	
19W46	18 07 32.42 0.11	-28 03 37.2 10.1	5.9	1.38	0.21	
19W47	18 07 52.09 0.10	-28 09 11.3 9.3	5.7 0.6	1.19	0.16	
19W48	18 08 02.25 0.09	-28 22 14.6 7.4	11.5 1.0	1.92	0.31	
19W49	18 08 10.80 0.07	-28 00 30.2 3.8	27.8 0.7	1.07	0.10	
19W50	18 08 20.15 0.17	-27 46 32.6 17.1	4.7 0.9	1.96	0.31	PN
19W51	18 08 25.38 0.12	-28 23 15.0 11.6	7.1 1.0	1.94	0.30	PN
19W52	18 08 31.35 0.10	-28 04 54.9 8.9	5.0 0.5	1.00	0.01	
19W53	18 08 42.85 0.07	-28 11 29.9 3.6	47.3 1.0	1.10	0.12	PN
19W54	18 09 06.79 0.09	-27 36 41.7 8.2	34.1 4.3	6.30	0.49	
19W55	18 09 18.20 0.07	-28 01 15.8 3.4	324.0 9.3	1.28	0.12	
19W56	18 09 25.06 0.08	-27 58 54.1 5.0	16.0 0.9	1.43	0.23	PN
19W57	18 09 26.58 0.07	-28 28 20.9 3.8	115.5 8.7	4.21	0.44	
19W58	18 09 29.26 0.07	-28 04 07.9 3.6	45.5 1.6	1.40	0.22	
19W59	18 09 29.94 0.07	-28 37 14.7 3.6	625.8 61.6	14.87	0.58	
19W60	18 09 42.88 0.08	-28 00 56.7 4.7	22.0 1.1	1.71	0.28	
19W61	18 09 52.47 0.08	-28 02 41.5 4.4	31.8 1.7	1.94	0.31	
19W62	18 10 02.23 0.08	-27 52 42.2 5.0	36.1 2.8	3.12	0.40	
19W63	18 10 03.77 0.08	-28 23 58.3 5.0	55.7 5.2	5.15	0.47	
19W64	18 10 30.24 0.13	-27 55 27.8 13.1	16.9 2.9	5.25	0.47	
19W65	18 10 36.19 0.08	-28 10 46.3 4.4	75.2 6.8	5.43	0.47	
19W66	18 10 51.87 0.10	-28 05 37.1 9.7	37.5 5.4	8.25	0.52	
Field 5.						
19W67	17 23 40.04 0.12	-28 17 56.8 2.7	8.2 1.1	2.06	0.32	
19W68	17 23 40.96 0.13	-28 37 54.0 12.4	6.0 0.8	1.69	0.27	
19W69	17 23 49.14 0.12	-28 26 00.0 10.8	5.8 0.7	1.41	0.22	
19W70	17 23 54.25 0.14	-28 13 16.6 3.3	7.3 1.2	2.31	0.35	
19W71	17 23 57.70 0.09	-28 10 46.3 8.2	15.7 1.7	2.73	0.37	
19W72	17 24 10.50 0.12	-28 38 22.1 10.8	5.2 0.7	1.28	0.19	
19W73	17 24 10.59 0.07	-28 25 27.6 3.8	33.2 0.9	1.19	0.16	PN
19W74	17 24 15.57 0.08	-28 17 09.4 4.7	36.5 3.6	1.55	0.25	E
19W75	17 24 22.83 0.12	-28 49 28.2 11.6	8.2 1.2	2.16	0.33	
19W76	17 24 23.16 0.08	-28 28 39.9 4.4	17.4 0.6	1.06	0.09	PN
19W77	17 24 25.05 0.09	-28 56 16.6 7.8	25.3 2.8	4.14	0.44	
19W78	17 24 25.83 0.07	-20 13 00.3 3.8	46.2 2.3	1.89	0.30	
19W79	17 24 31.14 0.09	-28 56 50.5 5.0	47.9 4.2	4.34	0.45	
19W80	17 24 33.70 0.07	-28 38 22.2 3.8	24.1 0.8	1.14	0.14	
19W81	17 24 36.92 0.08	-28 11 43.4 8.2	11.4 1.1	2.00	0.32	
19W82	17 24 38.92 0.08	-28 48 33.1 5.0	36.4 1.9	1.92	0.30	
19W83	17 24 55.20 0.08	-28 39 55.0 5.0	13.1 0.7	1.19	0.16	
19W84	17 25 18.76 0.11	-28 43 36.2 6.7	255.7 24.0	1.50	0.24	D 67" 170°
19W85	17 25 20.08 0.11	-28 15 11.9 10.1	7.7 1.0	1.76	0.28	
19W86	17 25 32.10 0.13	-28 25 08.6 12.4	4.8 0.6	1.27	0.19	PN
19W87	17 25 35.02 0.12	-28 25 21.9 10.8	5.2 0.7	1.30	0.19	
19W88	17 25 50.16 0.09	-28 38 47.8 7.1	11.0 1.0	1.67	0.27	
19W89	17 25 53.10 0.09	-28 46 09.6 5.7	22.4 1.8	2.50	0.36	
19W90	17 26 30.50 0.17	-28 38 01.4 16.7	6.8 1.4	3.17	0.40	PN
19W91	17 26 43.42 0.10	-28 25 37.4 8.5	21.4 2.5	4.00	0.43	
Field 6.						
19W92	17 43 20.53 0.08	-29 07 37.7 5.3	24.4 2.0	2.95	0.39	
19W93	17 43 39.93 0.08	-29 21 27.5 5.3	15.5 1.0	1.92	0.31	
19W94	17 43 42.87 0.08	-28 59 52.3 7.1	26.5 2.1	2.98	0.39	
19W95	17 43 44.11 0.13	-29 26 52.8 7.8	36.1 3.9	2.17	0.33	E 4′.9 0°
19W96	17 43 56.58 0.08	-28 44 56.2 4.7	143.8 15.5	13.01	0.57	
19W97	17 44 01.34 0.08	-29 28 18.1 3.8	35.2 1.7	1.85	0.30	
19W98	17 44 07.26 0.07	-29 26 37.1 3.6	62.5 3.3	1.61	0.26	
19W99	17 44 08.72 0.08	-29 10 48.8 5.0	12.4 0.7	1.34	0.21	
19W100	17 44 28.60 0.08	-29 14 42.6 4.7	11.3 0.5	1.09	0.12	
19W101	17 44 42.80 0.08	-28 50 50.8 5.0	33.5 2.9	3.74	0.42	
19W102	17 44 49.95 0.07	-28 55 25.9 3.8	37.4 2.1	2.33	0.35	
19W103	17 44 59.59 0.07	-28 55 54.1 5.0	199.4 10.1	2.22	0.34	
19W104	17 45 01.92 0.08	-29 09 54.8 4.7	11.4 0.5	1.07	0.10	
19W105	17 45 09.67 0.08	-28 53 38.7 4.7	30.5 2.1	2.73	0.37	
19W106	17 45 16.82 0.08	-29 38 12.3 3.8	48.4 3.0	2.75	0.38	
19W107	17 45 18.00 0.08	-29 13 14.8 4.4	12.6 0.5	1.04	0.08	
19W108	17 45 27.66 0.09	-29 31 16.1 6.7	9.6 0.8	1.70	0.18	
19W109	17 45 34.69 0.07	-29 06 44.4 3.6	45.0 1.4	1.32	0.20	
19W110	17 45 38.28 0.07	-28 51 47.4 3.6	499.0 52.0	3.81	0.43	E 0′.6
19W111	17 45 41.47 0.08	-29 26 04.5 4.7	15.5 0.8	1.43	0.22	
19W112	17 45 50.83 0.08	-29 11 17.7 5.0	12.8 0.7	1.32	0.20	
19W113	17 45 55.88 0.07	-29 22 52.8 3.6	238.4 8.3	1.46	0.23	
19W114	17 46 03.04 0.07	-28 51 25.3 3.6	127.4 10.5	5.34	0.47	
19W115	17 46 15	-28 48	2700 200	6.50	0.54	E 2′x 9′
19W116	17 46 16.80 0.08	-29 19 50.8 4.7	17.9 1.0	1.78	0.29	
19W117	17 46 20.10 0.08	-29 33 24.6 4.4	35.1 2.6	3.42	0.42	
19W118	17 46 21.08 0.08	-28 59 50.2 5.0	73.5 2.6	3.24	0.40	
19W119	17 46 46.75 0.08	-29 25 09.8 3.8	46.4 3.4	3.55	0.42	
19W120	17 46 55.12 0.09	-29 21 46.7 6.0	25.3 2.5	3.86	0.43	
19W121	17 47 03.50 0.07	-28 53 38.5 3.6	387.6 38.0	15.37	0.59	
19W122	17 47 12.89 0.10	-29 24 44.7 8.2	30.9 4.0	6.98	0.50	PN
19W123	17 47 13.63 0.09	-28 52 35.0 6.0	140.2 12.2	21.14	0.63	

* Column 7.
PN planetary nebulae
Esp extended; size; position angle
Ddp double; separation; position angle.

Table A2 Previously known sources

Name	α(1950)	δ(1950)	freq MHz	S(Jy)	size	beam
OTL 1725-287	17 25 19.08	-28 43 45.4	327	1.7	complex	120' x 4'
19W84	17 25 18.76	-28 43 36	1415	0.26		0'.3 x 2'
KES 54	17 37 07	-28 42	408	9	3'.6	1'.4 x 252' 2'.8 x 2'.8
19W40	17 36 57.56	-28 40 31.6	1415	0.19		0'.3 x 2'
BTD 0.4-0.8	17 46 24	-29 02	2650	8	7'	7'.4
19W118	17 46 21.08	-28 59 50.2	1415	1	1'.4	0'.3 x 2'
BTD 0.6-0.9	17 47 05	-28 53	2650	2.5		7'.4
19W121	17 47 03.50	-28 53 38.5	1415	0.34		0'.3 x 2'
NGC 6565	18 08 41.1	-28 11 18	5000	0.04		4'.5
19W53	18 08 42.85	-28 11 29.9	1415	0.047		0'.3 x 2'
OU-216	18 09 26	-28 21	1415	0.9		8'. x 45'
19 W55	18 09 18.20	-28 01 15.8	1415	0.32		
19 W57	18 09 26.58	-28 28 20.9	1415	0.11 } 1.06		0'.3 x 2'
19 W59	18 09 29.94	-28 37 14.7	1415	0.63		

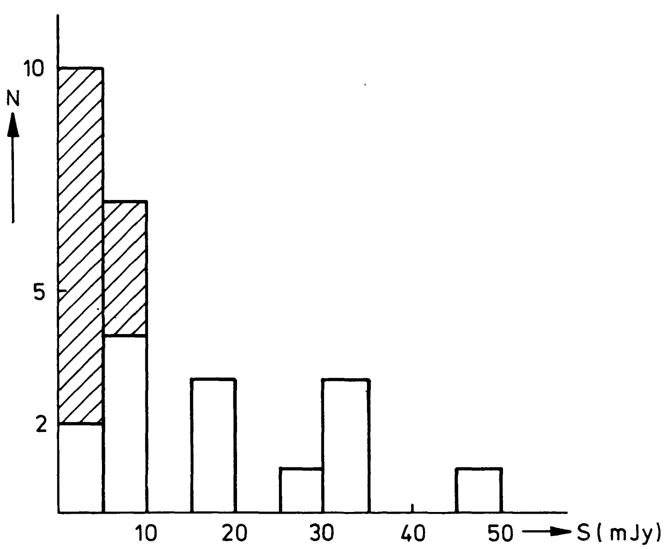

Figure 1 The distribution of flux densities of planetary nebulae near the galactic centre. The open area indicates observed sources, the hatched area includes upper limits.

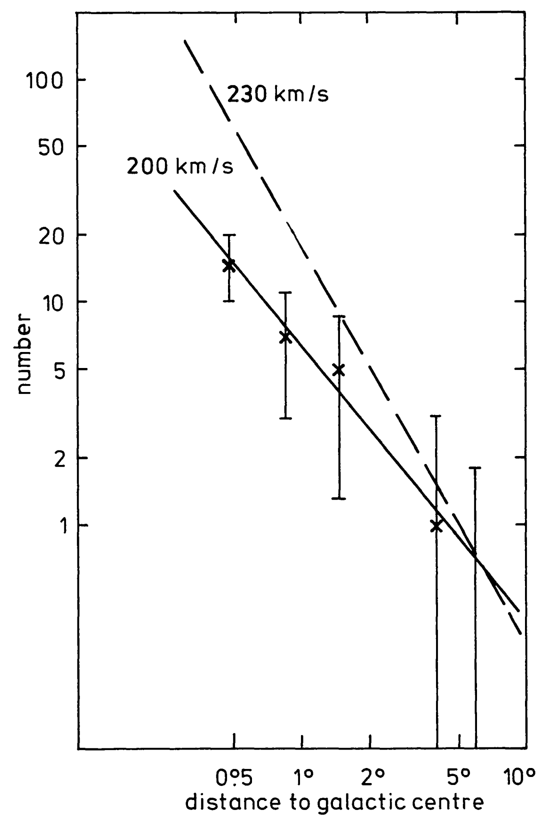

Figure 2 The distribution of sources near the galactic centre. The crosses indicate the number of sources brighter than 6.5 mJy (uncorrected for primary beam attenuation) within 0°.4 from the fieldcentre above the expected number of backgroundsources for a velocity dispersion of planetary nebulae near the galactic centre of 134 km s^{-1}. The full drawn and dashed lines indicate a circular velocity at $r = 200$ pc of 200 and 230 km s^{-1} respectively.